CHEMISTRY OF MATERIALS

VOLUME 20, NUMBER 17 SEPTEMBER 9, 2008

Communications

Programming Star-Mesogens toward the Formation of Columnar or Cubic Phases

Matthias Lehmann* and Michael Jahr

Institute of Chemistry, Chemnitz University of Technology,
Straße der Nationen 62, 09111 Chemnitz, Germany

Received May 14, 2008
Revised Manuscript Received July 15, 2008

Liquid crystalline (LC) phases combine the properties of anisotropic and fluid materials and therefore play a major role in nature,[1,2] optoelectronic devices,[3] and new tailor-made materials for plastic electronics.[4] However, LC properties can still not be predicted for newly designed mesogens.[5] Although a huge amount of work has been performed on nonconventional mesogens,[6] e.g., bolaamphiphiles,[7] dendrons, and dendrimers,[8] the hierarchical organization driven by nanosegregation and shape of the molecules can only be roughly estimated. Interesting examples are star-shaped mesogens with three arms because the free space between the individual arms should prevent an effective nanosegregation and thus the formation of mesophases. In contrast to our expectations, this mesogen family forms almost all types of mesophases from nematic, lamellar, columnar, to cubic phases.[6,9] Star-shaped structures based on oligobenzoate scaffolds and a phloroglucinol core have been shown recently to assemble in various columnar phases by optimization of space filling and nanosegregation of *E*-shaped conformers.[9,10] We became interested in non-C_3-symmetric mesogens, when we observed that the LC properties disappeared while the samples were heated to the isotropic phase. Gel permeation chromatography (GPC) and FD mass spectrometry give evidence for a transesterification process, which leads to mixtures of molecules of different size and symmetry; thus, eventually, materials do not exhibit any LC properties (see the Supporting Information). In the present investigation, we will show, that desymmetrisation of star-shaped mesogens leads to the formation of new self-assemblies for neat compounds. In the series of molecules with the same number and types of building blocks, the structure of the mesophase can be programmed, whereas the clearing temperature remains almost identical.

The synthesis of the non-C_3-symmetric oligobenzoates has been recently reported on the basis of a ABC building block

---

* Corresponding author. E-mail: matthias.lehmann@chemie.tu-chemnitz.de.

(1) (a) Hameley, I. W. *Introduction to Soft Matter*, 2nd ed.; Wiley: Chichester, U.K., 2007. (b) Hamley, I. W.; Castelletto, V. *Angew. Chem., Int. Ed.* **2007**, *46*, 4442; *Angew. Chem.* **2007**, *119*, 4524.

(2) Hoath, S.; Norlén, L. In *Bicontinous Liquid Crystals*; Taylor & Francis: Boca Raton, FL, 2005.

(3) Vicari, L., Ed. *Optical Applications of Liquid Crystals*; Institute of Physics Publishing: Bristol, U.K., 2003.

(4) (a) Kato, T.; Mizoshita, N.; Kishimoto, K. *Angew. Chem., Int. Ed.* **2006**, *45*, 38−68; *Angew. Chem.* **2006**, *118*, 45−74. (b) Bushby, R. J.; Lozman, O. R. *Curr. Opin. Colloid Sci.* **2002**, *7*, 343–354. (c) Sergeyev, S.; Pisula, W.; Geerts, Y. *Chem. Soc. Rev.* **2007**, *36*, 1902. (d) Laschat, S.; Baro, A.; Steinke, N.; Giesselmann, F.; Hägele, C.; Scalia, G.; Judele, R.; Kapatsina, E.; Sauer, S.; Schreivogel, A.; Tosoni, M. *Angew. Chem.* **2007**, *119*, 4916; *Angew. Chem., Int. Ed.* **2007**, *46*, 4832.

(5) Lehmann, M.; Lemaur, V.; Cornil, J.; Brédas, J.-L.; Goddard, S.; Grizzi, I.; Geerts, Y. *Tetrahedron* **2004**, *60*, 3283–3291.

(6) (a) Tschierske, C. *Ann. Rep. Prog. Chem., Sect. C* **2001**, *97*, 191, and references therein. (b) Tschierske, C. *Prog. Polym. Sci.* **1996**, *21*, 775. (c) Demus, D. *Liq. Cryst.* **1989**, *5*, 75. (d) Tschierske, C. *J. Mater. Chem.* **1998**, *8*, 1485–1508.

(7) Tschierske, C. *Chem. Soc. Rev.* **2007**, *36*, 1930.

(8) (a) Marcos, M.; Martín-Rapún, R.; Omenat, A.; Serrano, J.-L. *Chem. Soc. Rev.* **2007**, *36*, 1889, and references therein.

(9) Lehmann, M.; Jahr, M.; Donnio, B.; Graf, R.; Gemming, S.; Popov, I. *Chem.—Eur. J.* **2008**, *14*, 3562.

(10) (a) Lehmann, M.; Gearba, R. I.; Koch, M. H. J.; Ivanov, D. *Chem. Mater.* **2004**, *16*, 374. (b) Lehmann, M.; Gearba, R. I.; Koch, M. H. J.; Ivanov, D. *Mol. Cryst. Liq. Cryst.* **2004**, *411*, 397.

10.1021/cm8013094 CCC: $40.75

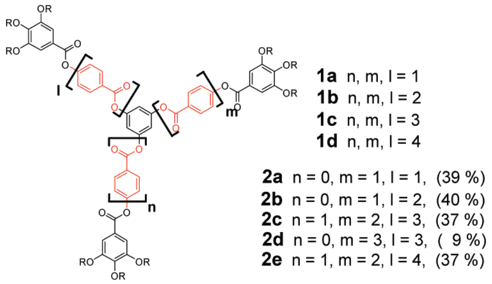

Figure 1. Star mesogens ($R = C_{12}H_{25}$): C_3-symmetric derivatives **1** and non-C_3-symmetric compounds **2** (Overall yields for five step synthesis).

Table 1. GPC Results

compd	M (g mol^{-1})	t_R (min)[a]
1a	2457.6	18.52
2b	2457.6	18.48
2c	2817.9	18.02
2d	2817.9	18.00
1b	2817.9	17.98
2e	2938.0	17.87[b]
1c	3178.2	17.55

[a] Values are measured with the addition of a standard (tribenzyl phloro-glucinol) with $t_R = 24.22$ min. [b] Value was measured under slightly different conditions and subsequently calibrated to the common standard.

with orthogonal protecting groups.[11] In a five-step esterification-deprotection procedure, the products could be prepared with an overall yield approaching 40%. Three non-C_3-symmetric products (**2b**, **2c**, **2e**) were obtained containing different numbers of repeating units in each oligobenzoate arm (Figure 1). Compound **2d** was isolated in a five-step synthesis as side product.[12] However, the C_2-symmetric star oligobenzoate **2a** was more conveniently prepared starting from the dibenzyl protected phloroglucinol. All materials were analyzed by ^{1}H, ^{13}C NMR, mass spectrometry, and elemental analysis. Results from GPC analysis are shown in Table 1.

GPC separates by size of molecules, which is a function of the molar mass.[13,14] Thus, mesogens with the same molecular mass appear to have similar retention times t_R; however, the difference in symmetry and consequently in shape result in slight differences in t_R, which are reproducible. The mixture of many different star-shaped molecules as formed during the transesterification reaction in the isotropic phase leads to a broad GPC curve when compared with single, neat compounds (see the Supporting Information). Transesterification is promoted by traces of water; therefore, materials **2** were all freeze-dried prior to the thermotropic investigations.

Table 2 summarizes the thermotropic properties of non-C_3-symmetric mesogens **2** compared to the symmetric stars **1** studied by differential scanning calorimetry (DSC), polarized optical microscopy (POM), and X-Ray diffraction (XRD). The phase transition temperatures increase with increasing number of repeating units. All molecules with the same number of oligobenzoate units clear in a similar temperature range, c.p. **1a** and **2b** as well as **1b**, **2c**, and **2d**; thus, transition temperatures mainly depend on the size of the mesogens. The transition entropies corresponding with transitions from the mesophase to the isotropic phase are much smaller for molecules **2** (4−6 J K^{-1} mol^{-1}) when compared with the C_3-symmetric mesogens **1** (8−16 J K^{-1} mol^{-1}). This points to a higher disorder in the packing of oligobenzoate scaffolds because of the lower symmetry of mesogens **2**. In the case of **2a** and **2c**, when there are no large differences of the arm lengths, the latter prevents the formation of the high-ordered low temperature columnar phases observed for oligobenzoates **1**. Cubic mesophases are formed when the dissimilarity in the number of repeating units is large (**2b**, **2d**, **2e**) as indicated by POM investigations. The cubic phases appear to be optical isotropic between cover slides or in a faceted LC drop (images A and B in Figure 2) and are highly viscous. Shear leads briefly to birefringence until self-healing recovers the materials original state (Figure 2C). The columnar phases show typical pseudofocal-conic textures (Figure 2D).

XRD was performed on aligned samples, which were fabricated by extrusion of fibers while being heated in the LC phase. Figure 3 presents typical XRD patterns in the columnar and cubic phases. The patterns of the columnar phases are characterized by equatorial reflections indicating the 2D columnar order, a halo corresponding to the liquidlike aliphatic chains and some meridional broad reflections on the halo indicating intracolumnar average distances. The reflections at the equator reveal reciprocal Bragg distances in the ratio of 1: $\sqrt{3}$: 2, which clearly points to hexagonal phases of the p6 mm plane group. The intracolumnar average distance amounts to 4.5 Å. The hexagonal parameters a_{hex} (**2a** (40.7 Å, 29 °C); **2c** (52.6 Å, 30 °C); **2e** (54.0 Å, 30 °C)) are almost identical to the one of the hexagonal phases of the corresponding symmetric molecules with the same or similar number of benzoate repeating units (**1a** (42.6 Å, 40 °C); **1b** (49.9 Å, 91 °C)), which point to *E*-shaped conformers self-assembling along the columns.[9,10] The set of four signals on the halo at the meridian (Figure 3A, bottom) is consistent with a tilt of mesogens versus the columnar axis. The XRD pattern of the shear aligned cubic LC phases of compounds **2b**, **2d**, and **2e** are typically observed for nonoriented powders (Figure 3B). However, slow cooling from the isotropic phases result in larger domains and thus, a number of distinct reflections are observed (see Supporting Information). The exclusive emergence of reflections at small angles in combination with an unstructured halo at wide angles confirm the LC character. The small angle reflections correspond to reciprocal Bragg distances in the ratio of $1:\sqrt{2}:\sqrt{3}:\sqrt{4}$ which is in agreement with cubic space groups (cp. Table 3). Compound **2e** reveals a transition from a cubic to a hexagonal phase evidenced by only three remaining reflections at 30 °C (Figure 3C).

The space groups of the cubic phases are not easy to determine because of the small number of reflections. Thus, primitive (P), face-centered (F), and body-centered (I) unit cells are in principle compatible with the sequence of ratios. According to earlier discussions of cubic phases in the series of structural different LC dendrons, the aggregation in the highest symmetry in centrosymmetric space groups is always preferred because of the structural disorder in the phases of

---

(11) Lehmann, M.; Jahr, M. *Org. Lett.* **2006**, *8*, 721.
(12) Jahr, M. Diplomarbeit (Master Thesis), Chemnitz University of Technology, Chemnitz, Germany, 2005.
(13) Meier, H.; Lehmann, M. *Chem.—Eur. J.* **2000**, *6*, 2462.
(14) Dawkins, J. V. *Pure Appl. Chem.* **1979**, *51*, 1473.

Table 2. Thermotropic Properties of Non-Symmetric Star-Shaped Mesogens 2 and C_3-Symmetric Derivatives 1

	phase transition temperatures (°C)/transition enthalpies (kJ/mol)[a]		phase transition temperatures (°C)/transition enthalpies (kJ/mol)[a]
2a (2)[c]	$\mathbf{Col_{hd}}$ 36/5.6 **I**	**1a** (3)[c]	$\mathbf{Cr_{borh}}$ 55/32.7 (**g** 20 (T_g) $\mathbf{Col_h}$ 53/5.5) **I**[d]
2b (3)[c]	**Cub** 51/1.6 **I**		
2c (6)[c]	$\mathbf{Col_{hd}}$ 84/2.0 **I**	**1b** (6)[c]	$\mathbf{Col_{borh}}$ 79/11.6 $\mathbf{Col_h}$ 98/3.0 **I**[d]
2d (6)[c]	**g** 38 **Cub** 98/1.7 **I**		
2e (7)[c]	$\mathbf{Col_{hd}}$ 45/-[b] **Cub** 128/2.0 **I**	**1c** (9)[c]	$\mathbf{Col_{borh}}$ 170/10.1 $\mathbf{Col_h}$ 172/5.4 **I**[d]

[a] Values are given for the 2nd DSC heating cycle at a heating rate of 10 °C/min. [b] Transition was only observed by POM and X-Ray diffraction. [c] Total number of the benzoate repeating units in the mesogens. [d] Data from ref 9. Col columnar mesophases, Cub cubic mesophases, g LC glass, Cr crystalline phase, h hexagonal, hd hexagonal disordered, borh body-centered orthorhombic.

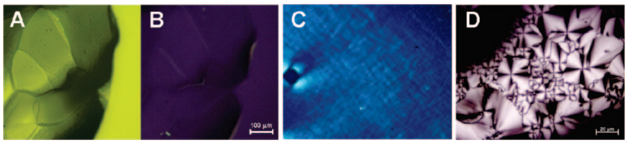

Figure 2. (A) Faceted drop of **2d** in its cubic phase at 81 °C. (B−D) Textures between crossed polarizers. (B) Optical isotropic texture of the faceted drop in A. (C) Birefringence of **2d** at 70 °C after mechanical stress. (D) Pseudofocal-conic texture of **2c** at 85 °C.

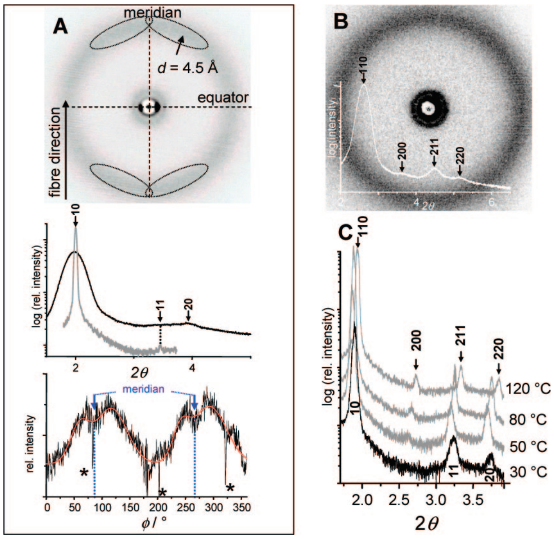

Figure 3. X-Ray diffraction of mesogens **2**. (A) Top, diffraction pattern of **2c** in the Col_h phase at 75 °C; middle, integration along the equator; WAXS (wide-angle X-ray scattering, black line), SAXS (small-angle X-ray scattering, gray line); bottom: integration of the halo along the azimuthal angle ϕ (black) and the fit curve (red). The maxima in the direction of the meridian can be attributed to the intracolumnar average separations of the oligobenzoate core; * signals originating from the suspensions of the beam stop. The observable splitting of these maxima points to a tilt of the mesogens versus the column axis. (B) Diffraction pattern of the cubic phase of **2b**. (C) Temperature-dependent SAXS patterns and indexation for **2e**: transition from a cubic to a Col_h phase.

thermotropic liquid crystals.[15,16] We focus further discussion to micellar phases in the *Pm3m, Pm3n*, *Fm3m*, and *Im3m* space groups, for which the indexations are given in Table 3. According to the reflection conditions in each space group, variations in indexation, cell parameters, number Z of mesogens per unit cell,[17] and number of micelles are given. Each micelle can be regarded as a inner oligobenzoate spherical core surrounded by a continuum of aliphatic chains, because the flexible peripheral chains constitute major portions of the mesogens, i.e., 64−73%. The volume of the oligobenzoate part of a single micelle (V_{core}) in a specific space group can be calculated with the experimental results of the unit cell ($V_{unit\ cell} = a^3$, number Z of molecules per unit cell), the known volume of aliphatic chains[18] and the number of micelles n per unit cell: $V_{core} = (V_{unit\ cell} - ZV_{chain\ per\ molecule})/n$. The radius r_{core} of this spherical volume for each space group is collected in Table 3. Only the values calculated for the body-centered *Im3m* space group are in agreement with the radii r_{mol} obtained from molecular models (last column of Table 3).

Table 3. X-Ray Results for the Cubic Phases

no.	d_{exp} (Å)[b]	n[a]	Z/n[a]	space group[b]	a (Å)	r_{core} (Å)	r_{mol} (Å)
2b (45 °C)	33.8, 24.0, 19.3, 16.8	1	9	*Pm3m*	33.8	13.7	15.6
		8	3	*Pm3n*	47.7	7.7	
		4	19	*Fm3m*	67.5	13.7	
		2	13	*Im3m*	47.7	15.3	
2d (80 °C)	41.8, 29.8, 24.4, 21.0	1	16	*Pm3m*	42.2	18.4	20.0
		8	6	*Pm3n*	59.7	10.3	
		4	31	*Fm3m*	84.0	18.3	
		2	23	*Im3m*	59.7	20.7	
2e (120 °C)	45.4, 32.2, 26.4, 22.9	1	19	*Pm3m*	45.5	20.1	24.0
		8	7	*Pm3n*	64.4	11.3	
		4	38	*Fm3m*	91.1	20.1	
		2	27	*Im3m*	64.4	22.6	

[a] n, Number of micelles per unit cell; Z/n, number of molecules per micelle. [b] Indexation for *Pm3m* (100, 110, 111, 200), *Pm3n*, *Im3m* (110, 200, 211, 220), *Fm3m* (200, 220, 222, 400).

A model visualizing the possible conformers in the hexagonal and the cubic phase for **2e** is given in Figure 4. As shown recently the aggregation in columnar phases can be realized by almost planar, *E*-shaped conformers. In the case of nonsymmetric mesogens, such conformers can be formed by folding successively the longer arms around the phloroglucinol core, comparable to a water fountain. Micelles can be best built from molecules with a cone shape. These are easily obtained when the longest arm folds behind the plane of the molecule.

In principle, bicontinous instead of micellar phases would also explain the results, because the oligobenzoates are able

---

(15) Coco, S.; Cordovilla, C.; Donnio, B.; Espinet, P.; García-Casas, M. J.; Guillon, D. *Chem.*—*Eur. J.* **2008**, *14*, 3544.

(16) (a) Yeardley, D. J. P.; Ungar, G.; Percec, V.; Holerca, M. N.; Johansson, G. *J. Am. Chem. Soc.* **2000**, *122*, 1684. (b) Percec, V.; Holerca, M. N.; Uchida, S.; Cho, W.-D.; Ungar, G.; Yeardley, D. J. P. *Chem.*—*Eur. J.* **2002**, *8*, 1106. (c) Balagurusamy, V. S. K.; Ungar, V.; Percec, V.; Johansson, V. *J. Am. Chem. Soc.* **1997**, *119*, 1539.

(17) The number of molecules in the unit cell is calculated by $Z = a^3/V_M$. V_M is the molecular volume. A molecular volume for crystalline material was estimated according to Immirzi, A.; Perini, B. *Acta Crystallogr., Sect. A* **1977**, *33*, 216–218. The obtained value was corrected by a factor using the experimental dilatometry data from ref 9.

(18) Donnio, B.; Heinrich, B.; Allouchi, H.; Kain, J.; Diele, S.; Guillon, D.; Bruce, D. W. *J. Am. Chem. Soc.* **2004**, *126*, 15258.

(19) Liu, B.; Zahang, X. Y.; Yang, X. Z. *Chin. Chem. Lett.* **1992**, *3*, 663.

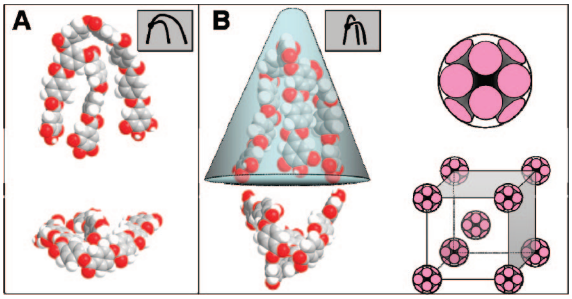

Figure 4. Molecular models omitting aliphatic chains for clarity. (A) *E*-shaped conformer forming columnar phases. (B) Cone-shaped conformer assembling in cubic phases and model of micelle and phase formation.

to generate both planar and cone shaped conformers. Further details in favor for a micellar phase originate from the phase sequence L (lamellar; **1** ($n,m,l = 000$))[19]−Col$_h$(**2a** ($n,m,l = 110$)−Cub(**2b** ($n,m,l = 012$) with increasing oligobenzoate segments and the fact that for **2b**, the ratio between oligobenzoate core and the peripheral aliphatic chain volume still amounts to 26:74. This is in accordance with conventional phase diagrams, where the cubic phase in the sequence is known to be micellar.[6] However, mesogens with the same ratio of benzoate core to aliphatic chain volume, e.g., **1b**, **2c**, **2d**, present a phase transition to a cubic phase, which clearly depends only on the desymmetrization. More detailed analyses of the cubic phases by synchrotron X-ray diffraction, AFM, and dielectric spectroscopy are in progress.

In conclusion, non-C_3-symmetric star-shaped mesogens show that mesomorphism of star-shaped oligobenzoates depend on the symmetry of the core, which can be manipulated by varying the number of benzoate units in each arm. Even with the same number of repeating units, i.e., the same ratio of oligobenzoate core to aliphatic chain volume, the mesomorphism and polymorphism can be controlled between columnar and cubic phases. The aggregation in such phases is explained by folding of the oligobenzoate scaffold.

Acknowledgment. We thank Prof. H. Meier, A. Oehlhof and Dr. N. Hanold for the elemental analysis and FD mass spectra completed at the University of Mainz, Prof. J. Gutmann and M. Bach for the possibility to measure XRD at the MPI for Polymer Research Mainz, and the German Science Foundation (DFG) and the Bundesministerium für Bildung and Forschung (BMBF) for their financial support.

Supporting Information Available: Experimental details and evidence for transesterification procedure (PDF). This material is available free of charge via the Internet at http://pubs.acs.org.

CM8013094